



Supplement of

Contribution of intermediate-volatility organic compounds from on-road transport to secondary organic aerosol levels in Europe

Stella E. I. Manavi and Spyros N. Pandis

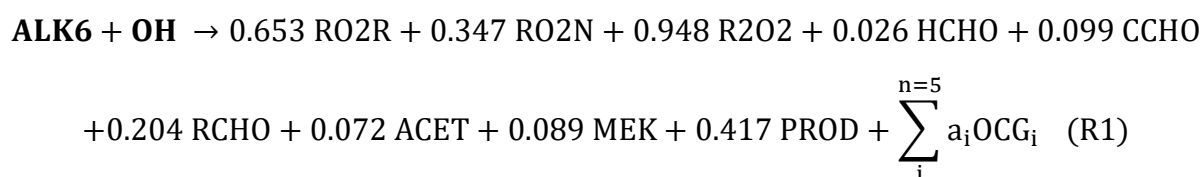
Correspondence to: Spyros N. Pandis (spyros@chemeng.upatras.gr)

The copyright of individual parts of the supplement might differ from the article licence.

S1 Lumped IVOC gas-phase chemistry and the SOA-iv parametrisation in PMCAMx-iv.

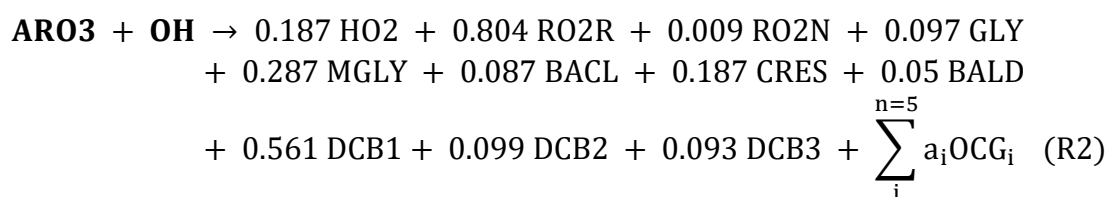
In PMCAMx-iv, all seven lumped IVOC species react individually in the gas-phase with the hydroxyl radical. These seven oxidation reactions lead to the formation of volatile products, which remain in the gas-phase, and lower volatility products, which partition to the aerosol phase and form SOA-iv. For the introduction of these seven reactions to the existing SAPRC gas-phase mechanism, it is assumed that their volatile products and their reaction rate constants are the same as the ones used to simulate OH radical reactions of larger VOCs, which are part of the pre-existing mechanism.

For the four lumped alkane species (ALK6, ALK7, ALK8 and ALK9), the oxidation reactions are based on the reaction of ALK5 with the hydroxyl radical. For example,



where, RO2R is the organic peroxy radical converting NO to NO₂ with HO₂ production, RO2N is the organic peroxy radical converting NO to organic nitrate, R2O2 is the organic peroxy radical converting NO to NO₂, HCHO is formaldehyde, CCHO is acetaldehyde, RCHO represents the higher aldehydes (based on propionaldehyde), ACET is acetone, MEK is methyl ketone, PROD represents other organic products, a_i is its NO_x-dependent mass-based yield and OCG_i is the *i*th oxygenated condensable lower volatility product which can partition to the aerosol phase (all seven new lumped species contribute to the formation of the same five lower volatility products). The reaction rate constant for reaction (R1) is assumed to have a value of 1.4 × 10⁴ ppm⁻¹ min⁻¹.

For the PAHs species (PAH1 and PAH2) and the new aromatic species (ARO3), their reactions are based on the reaction of ARO2 with the hydroxyl radical. For example,



where, HO2 is the hydroperoxyl radical, GLY is glyoxal, MGLY is methylglyoxal, BACL is biacetyl, CRES is cresol, BALD is benzaldehyde and DCB1-DCB3 represent three different aromatic ring-opening dicarbonyl products. The reaction rate constant for reaction (R2) is assumed to have a value of 3.9 × 10⁴ ppm⁻¹ min⁻¹.

The five lower volatility products have respectively an effective saturation concentration of 0.1, 1, 10, 100 and 10³ μg m⁻³. Each of the lower volatility products follows a partitioning reaction (R3) forming SOA-iv products with the corresponding volatility.



For all seven lumped species, the NO_x dependent stoichiometric yields are estimated based on recent experimental data.

S2 Evaluation criteria equations

The normalized mean bias (NMB), the normalized mean error (NME), the mean bias (MB), the mean absolute gross error (MAGE), the fractional bias (FBIAS), and the fractional error (FERROR) were calculated for the results of all eight simulations.

$$NMB = \frac{\sum_{i=1}^n (P_i - O_i)}{\sum_{i=1}^n O_i} \quad (1)$$

$$NME = \frac{\sum_{i=1}^n |P_i - O_i|}{\sum_{i=1}^n O_i} \quad (2)$$

$$MB = \frac{1}{n} \sum_{i=1}^n (P_i - O_i) \quad (3)$$

$$MAGE = \frac{1}{n} \sum_{i=1}^n |P_i - O_i| \quad (4)$$

$$FBIAS = \frac{2}{n} \sum_{i=1}^n (P_i - O_i) / (P_i + O_i) \quad (5)$$

$$FERROR = \frac{2}{n} \sum_{i=1}^n |P_i - O_i| / (P_i + O_i) \quad (6)$$

Table S1: Average percent contributions of IVOCs emitted from on-road diesel and gasoline vehicles to the formation of PM_{2.5} OA and SOA over 44 European capital cities for May 2008. The mean ground-level concentrations of SOA and OA in $\mu\text{g m}^{-3}$ are included in the parenthesis.

European Capital	PMCAMx-iv	
	SOA (%)	OA (%)
Tirana	3.9 (2.27)	2.6 (3.45)
Yerevan	7.5 (0.28)	1.6 (1.33)
Vienna	4.7 (2.08)	2.7 (3.55)
Baku	6.4 (0.32)	1.5 (1.35)
Minsk	3.7 (2.92)	2.3 (4.65)
City of Brussels	3.9 (1.26)	2.2 (2.27)
Sarajevo	3.8 (1.32)	2.2 (2.33)
Sofia	7.2 (1.42)	4.2 (2.44)
Zagreb	4.2 (1.62)	2.4 (2.8)
Nicosia	7.0 (1.24)	3.3 (2.64)
Prague	4.3 (2.37)	2.7 (3.72)
Copenhagen	3.4 (2.78)	2.2 (4.26)
Tallinn	3.3 (2.03)	1.6 (4.32)
Helsinki	5.5 (0.54)	2.0 (1.48)
Paris	2.9 (1.44)	1.2 (3.38)
Tbilisi	3.3 (1.18)	1.5 (2.67)
Berlin	4.5 (2.93)	1.8 (7.16)
Athens	3.9 (2.8)	2.4 (4.48)
Budapest	7.0 (0.42)	2.2 (1.38)
Dublin	7.2 (1.84)	3.6 (3.72)
Rome	4.0 (1.91)	2.6 (2.99)
Prizren	5.3 (2.02)	3.3 (3.24)
Riga	4.0 (1.77)	2.5 (2.9)
Vilnius	5.0 (1.97)	3.0 (3.28)
Luxembourg	3.8 (1.18)	2.1 (2.15)
Valletta	4.4 (1.45)	2.6 (2.48)
Chisinau	3.5 (2.41)	2.1 (4.05)
Podgorica	3.3 (1.41)	1.6 (2.95)
Amsterdam	5.8 (1.48)	3.4 (2.57)
Oslo	3.8 (1.21)	2.1 (2.24)
Warsaw	3.9 (1.05)	1.8 (2.26)
Lisbon	3.7 (1.28)	2.1 (2.3)
Skopje	3.5 (2.9)	2.0 (5.14)
Bucharest	2.6 (1.21)	1.1 (2.9)
Moscow	4.7 (1.63)	2.7 (2.82)
Belgrade	4.0 (0.59)	1.6 (1.51)
Bratislava	4.8 (1.39)	2.8 (2.38)
Ljubljana	8.8 (1.91)	4.0 (4.23)
Madrid	3.8 (1.63)	2.4 (2.61)
Stockholm	4.7 (2.11)	3.0 (3.28)

Bern	3.8 (1.83)	2.4 (2.85)
Ankara	2.7 (1.19)	1.3 (2.47)
Kyiv	7.3 (0.82)	3.0 (1.96)
London	6.6 (1.56)	3.5 (2.93)

Table S2: Prediction skill metrics of PMCAMx, PMCAMx-iv and the six sensitivity tests against AMS hourly ground measurements of PM₁ OA concentration from the four measuring stations that were part of the EUCAARI campaign in May 2008.

Test name	Mean Observed ($\mu\text{g m}^{-3}$)	Mean Predicted ($\mu\text{g m}^{-3}$)	MB ($\mu\text{g m}^{-3}$)	MAGE ($\mu\text{g m}^{-3}$)	NMB	NME	FBIAS	FERROR
Cabauw								
VBS-scheme (PMCAMx)	4.1	4.6	0.7	1.6	16.5	37.9	0.2	0.4
Base case (PMCAMx-iv)	4.1	4.7	0.7	1.6	17.9	38.4	0.2	0.4
Lumped IVOC emissions $\times 2$	4.1	4.8	0.9	1.6	21.3	39.8	0.2	0.4
No gas-phase chemistry	4.1	4.7	0.7	1.6	17.7	38.2	0.2	0.4
Multigenerational aging	4.1	4.8	0.9	1.6	21.3	39.8	0.2	0.4
MW effect	4.1	4.8	0.9	1.6	20.7	39.6	0.2	0.4
ΔH effect	4.1	4.7	0.8	1.6	19.5	39.1	0.2	0.4
Different yields	4.1	4.7	0.7	1.6	18.1	38.5	0.2	0.4
Finokalia								
VBS-scheme (PMCAMx)	2.5	2.4	0.1	0.8	2.7	31.4	0.1	0.3
Base case (PMCAMx-iv)	2.5	2.4	0.1	0.8	4.0	31.4	0.1	0.3
Lumped IVOC emissions $\times 2$	2.5	2.5	0.2	0.8	7.5	32.1	0.1	0.3
No gas-phase chemistry	2.5	2.4	0.1	0.8	4.0	31.4	0.1	0.3
Multigenerational aging	2.5	2.6	0.3	0.9	13.4	34.5	0.1	0.4
MW effect	2.5	2.5	0.2	0.8	7.5	32.1	0.1	0.3
ΔH effect	2.5	2.4	0.1	0.8	5.4	31.5	0.1	0.3
Different yields	2.5	2.4	0.1	0.8	4.5	31.5	0.1	0.3
Mace Head								
VBS-scheme (PMCAMx)	2.3	2.5	-0.1	1.0	-3.9	41.1	-0.2	0.5
Base case (PMCAMx-iv)	2.3	2.5	-0.1	1.0	-3.8	41.3	-0.2	0.5
Lumped IVOC emissions $\times 2$	2.3	2.5	0.0	1.0	-1.9	41.7	-0.2	0.5

No gas-phase chemistry	2.3	2.5	-0.1	1.0	-3.9	41.3	-0.2	0.5
Multigenerational aging	2.3	2.6	0.0	1.0	0.2	42.1	-0.2	0.5
MW effect	2.3	2.5	0.0	1.0	-1.9	41.7	-0.2	0.5
ΔH effect	2.3	2.5	-0.1	1.0	-2.3	41.6	-0.2	0.5
Different yields	2.3	2.5	-0.1	1.0	-3.7	41.3	-0.2	0.5
Melpitz								
VBS-scheme (PMCAMx)	5.1	3.8	-1.2	1.8	-23.3	34.2	-0.3	0.4
Base case (PMCAMx-iv)	5.1	3.8	-1.1	1.7	-21.8	33.8	-0.2	0.4
Lumped IVOC emissions $\times 2$	5.1	3.9	-1.0	1.7	-18.7	33.4	-0.2	0.4
No gas-phase chemistry	5.1	3.8	-1.1	1.7	-21.7	33.7	-0.2	0.4
Multigenerational aging	5.1	4.0	-0.9	1.7	-17.4	33.5	-0.2	0.4
MW effect	5.1	3.9	-1.0	1.7	-19.0	33.4	-0.2	0.4
ΔH effect	5.1	3.9	-1.1	1.7	-20.7	33.3	-0.2	0.4
Different yields	5.1	3.8	-1.1	1.7	-21.4	33.7	-0.2	0.4

Table S3: Average percent contributions of on-road IVOCs to the formation of PM₁ OA concentrations over the four measuring stations were part of the EUCAARI campaign in May 2008. The contributions are calculated for all eight simulation cases.

Test name	Contribution to PM₁ OA (%)
Cabauw	
VBS-scheme (PMCAMx)	1.3
Base case (PMCAMx-iv)	2.2
Lumped IVOC emissions × 2	4.4
No gas-phase chemistry	2.2
Multigenerational aging	4.4
MW effect	4.3
ΔH effect	3.2
Different yields	2.3
Finokalia	
VBS-scheme (PMCAMx)	1.7
Base case (PMCAMx-iv)	2.9
Lumped IVOC emissions × 2	5.7
No gas-phase chemistry	2.9
Multigenerational aging	9.5
MW effect	5.8
ΔH effect	4.1
Different yields	3.2
Mace Head	
VBS-scheme (PMCAMx)	1.8
Base case (PMCAMx-iv)	2.0
Lumped IVOC emissions × 2	4.0
No gas-phase chemistry	2.0
Multigenerational aging	5.2
MW effect	4.1
ΔH effect	3.3
Different yields	2.2
Melpitz	
VBS-scheme (PMCAMx)	1.4
Base case (PMCAMx-iv)	2.4
Lumped IVOC emissions × 2	4.8
No gas-phase chemistry	2.4
Multigenerational aging	5.4
MW effect	4.7
ΔH effect	3.3
Different yields	2.6

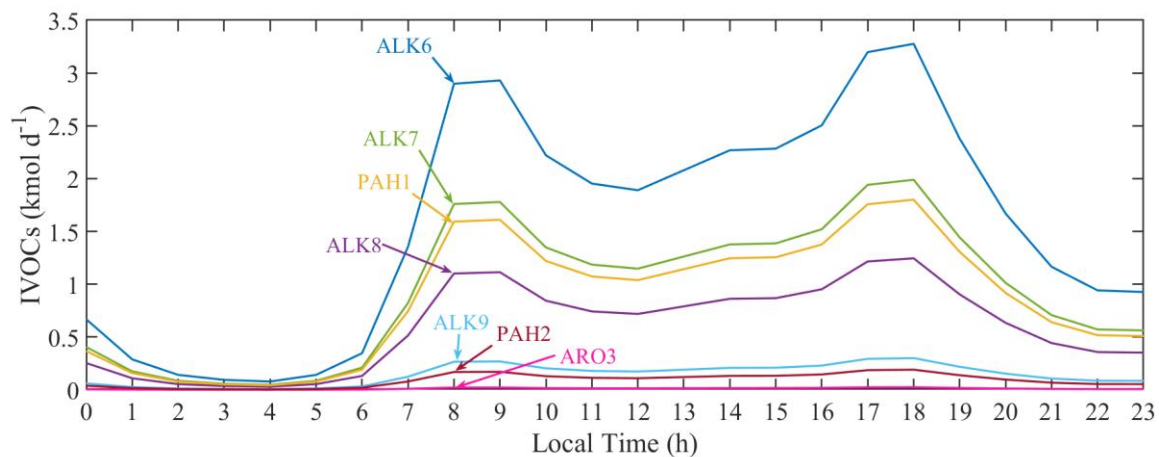


Figure S1: Average diurnal profiles of the on-road diesel and gasoline vehicle emissions of the seven lumped IVOC species over Paris for May 2008.

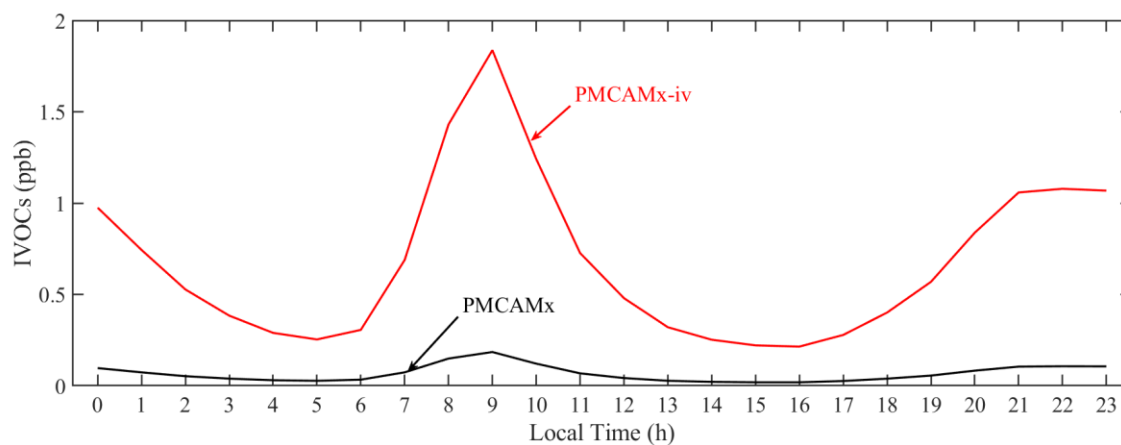


Figure S2: Average diurnal profiles for the ground-level concentrations of on-road transportation IVOCs over Paris as predicted by PMCAMx (sum of the four surrogate species) and PMCAMx-iv (sum of the seven lumped IVOC species) for May 2008.

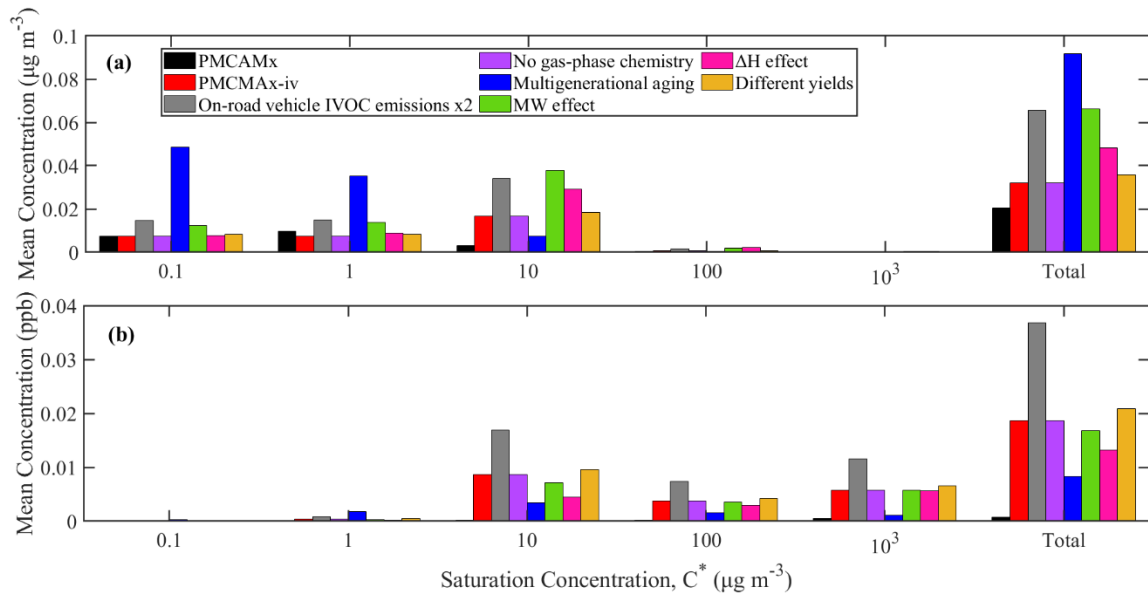


Figure S3: Domain-averaged ground-level concentrations of the SOA-iv products (a) in the aerosol phase and (b) in the gas-phase predicted by PMCAMx, PMCAMx-iv and by the different sensitivity tests for the May 2008 simulations over Europe.

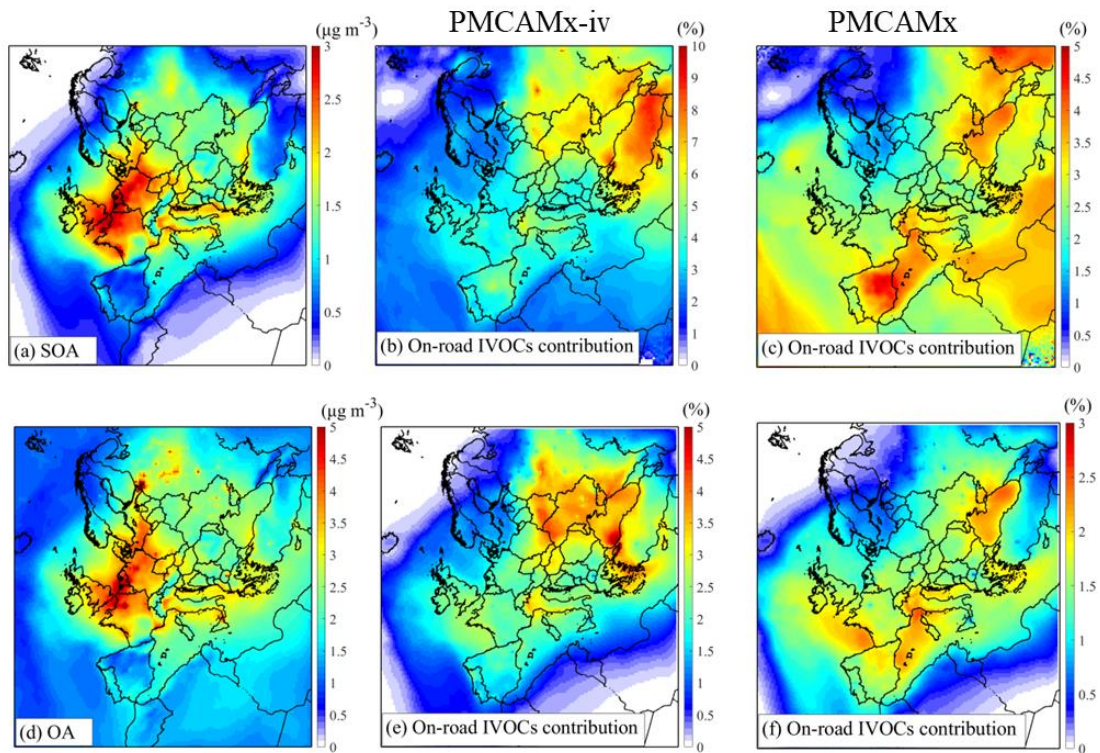


Figure S4: Estimated averaged ground-level $\text{PM}_{2.5}$ concentrations of (a) SOA and (d) OA concentrations and the corresponding contributions from on-road diesel and gasoline vehicles IVOCs over Europe for May 2008 using (b,e) PMCAMx-iv and (c,f) PMCAMx-iv.

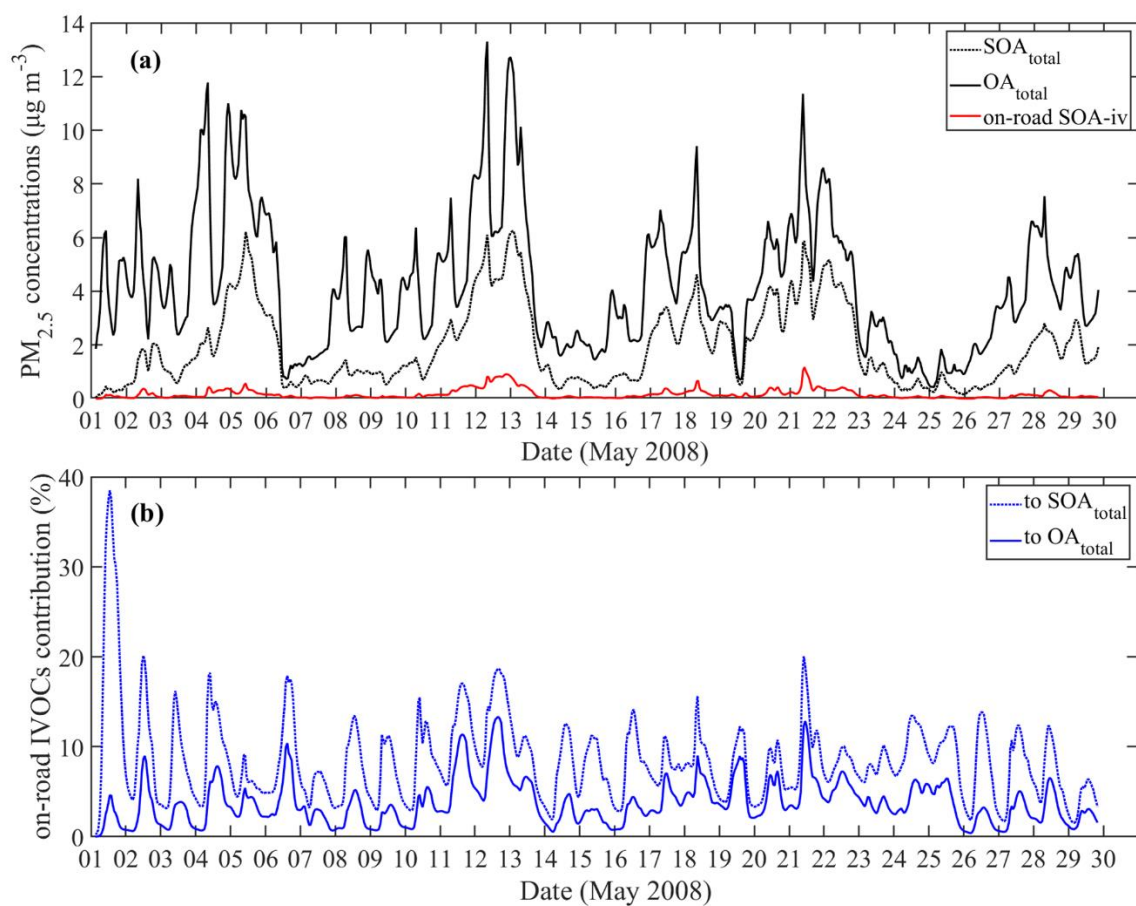


Figure S5: (a) PMCAMx-iv estimated hourly-averaged ground-level concentrations of PM_{2.5} SOA_{total}, OA_{total} and on-road SOA-iv over Moscow and (b) the contributions of on-road IVOCs to the total SOA and OA concentrations for May 2008.

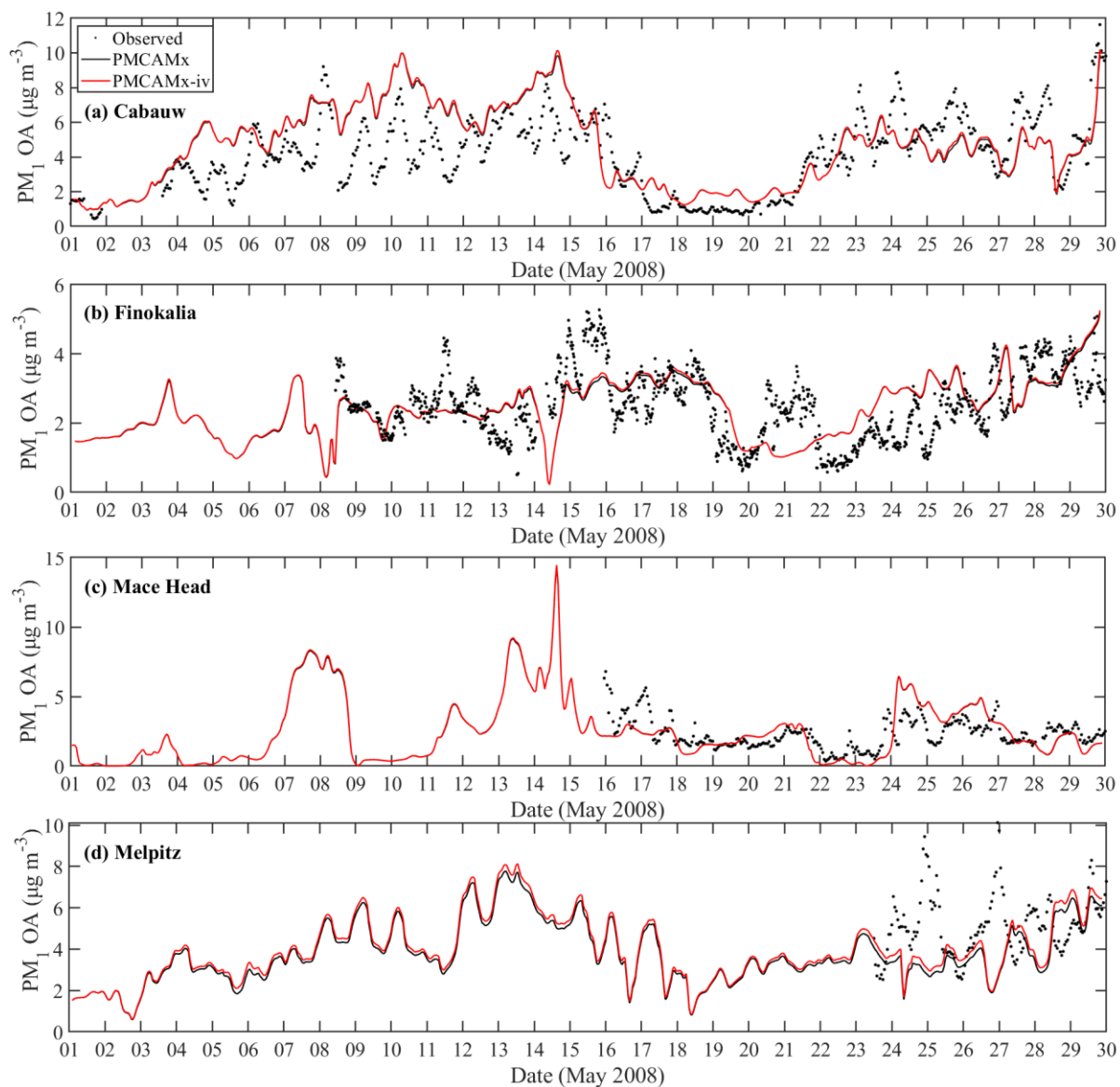


Figure S6: Comparisons of the PMCAMx and PMCAMx-iv predictions with the measurements of PM₁ OA (in $\mu\text{g m}^{-3}$) taken at the four EUCAARI measurement sites in May 2008 ((a) Cabauw, (b) Finokalia, (c) Mace Head, (d) Melpitz).

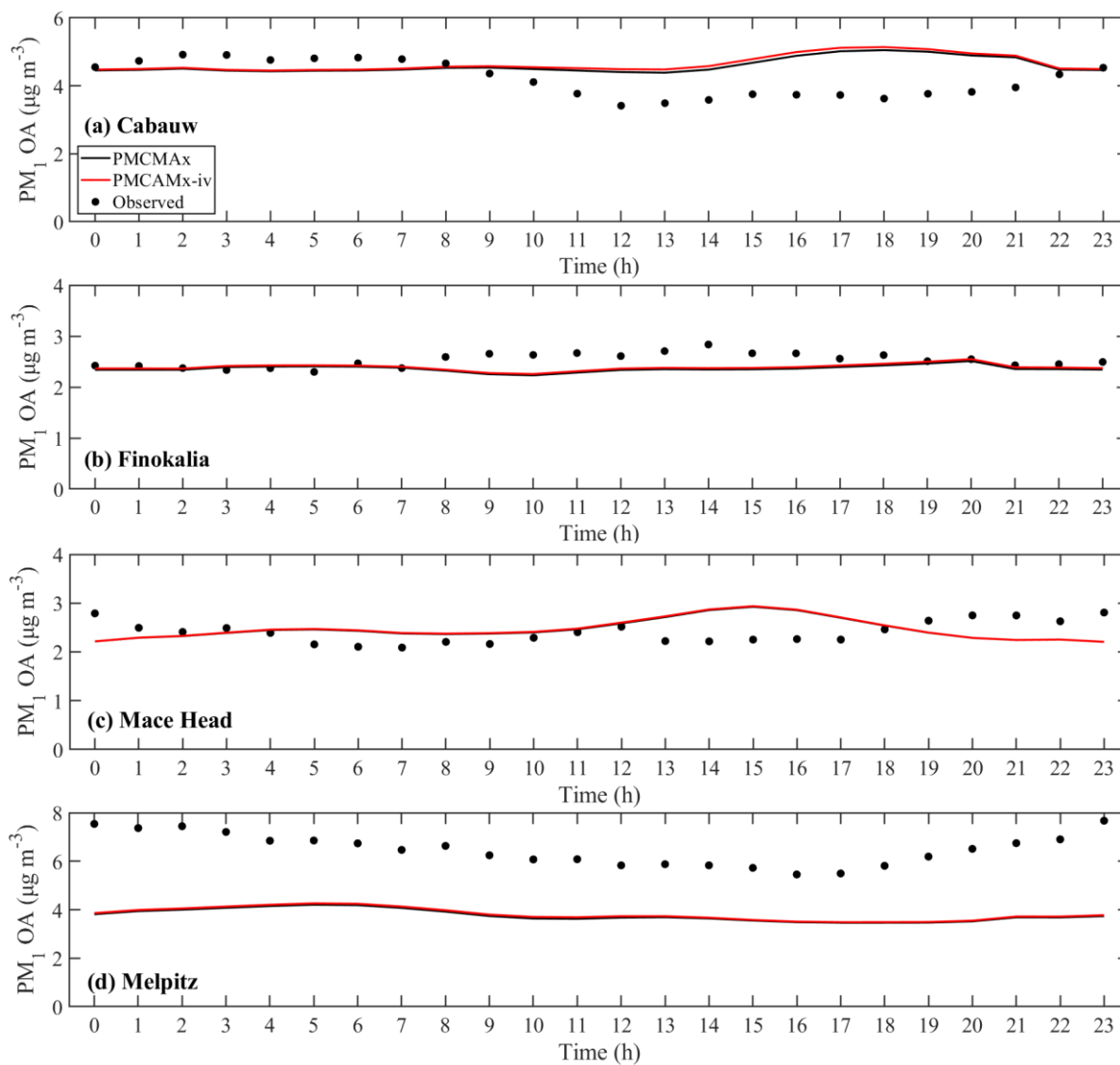


Figure S7: Average diurnal profiles of $PM_{1\text{ OA}}$ concentrations over the four EUCAARI measuring sites for May 2008 ((a) Cabauw, (b) Finokalia, (c) Mace Head, (d) Melpitz).

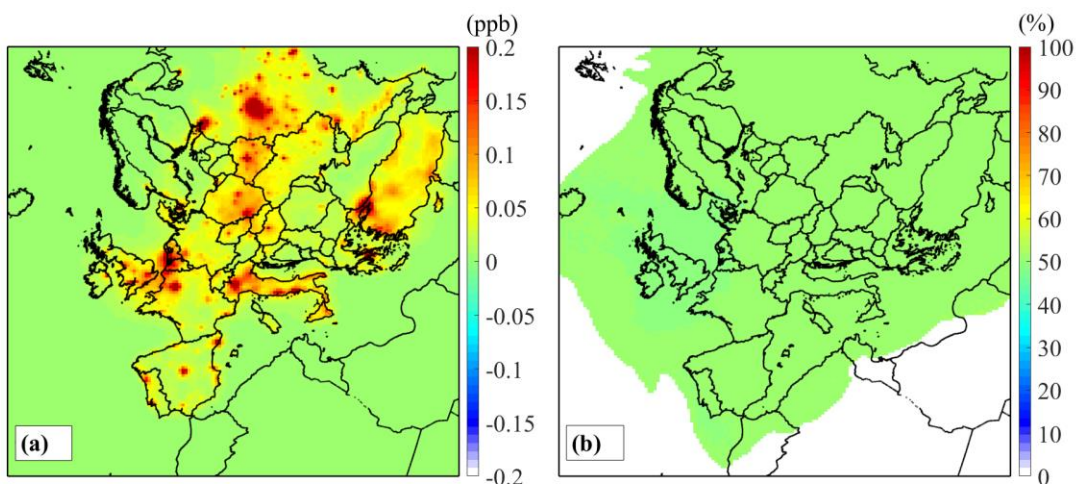


Figure S8: (a) Absolute and (b) percentage differences between the average ground-level concentrations of the sum of the seven lumped IVOC species that are predicted in the “base case” and the “IVOC emissions $\times 2$ ” simulations.

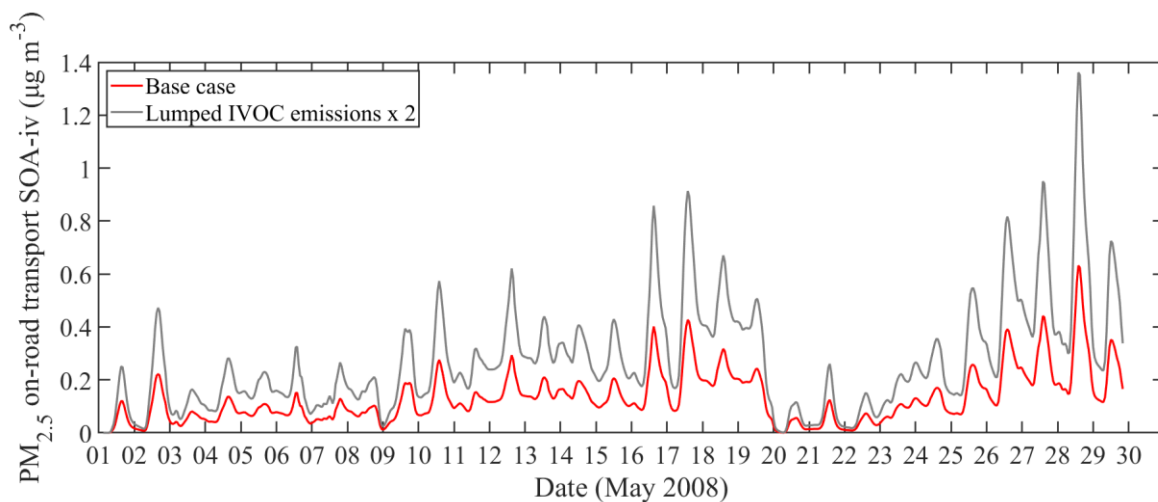


Figure S9: $PM_{2.5}$ hourly-averaged timeseries for the predicted ground-level concentrations of on-road transport SOA-iv by the “VBS scheme”, the “base case” and the “lumped IVOC emissions $\times 2$ ” simulations over the city of Athens for May 2008.

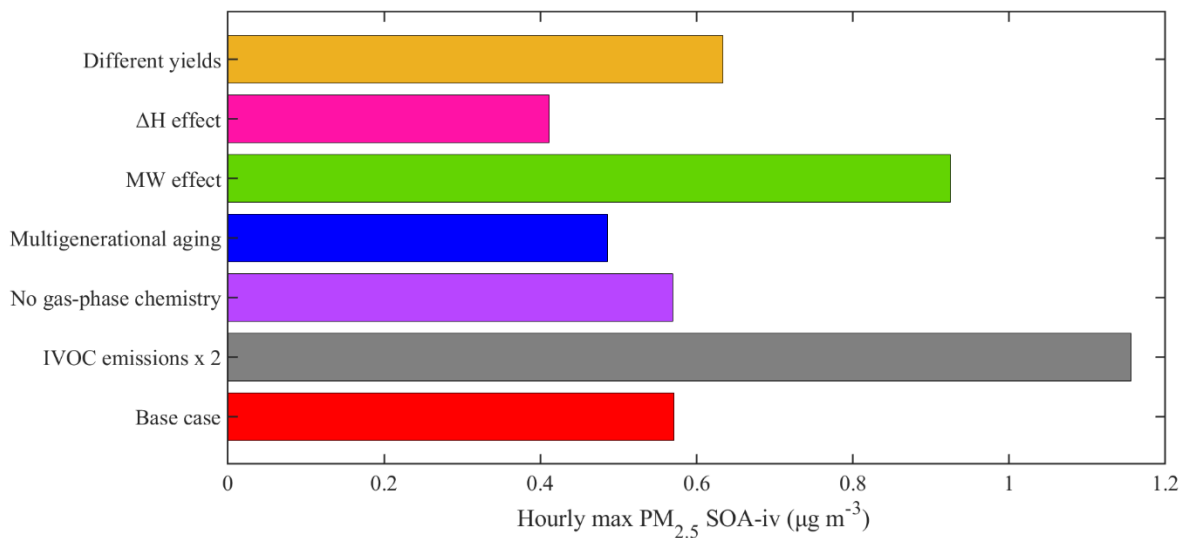


Figure S10: The maximum hourly $PM_{2.5}$ SOA-iv concentrations for May 2008 over Paris as predicted by the “base case” and the six sensitivity tests of PMCAMx-iv. Not all max values are predicted to occur at the same time.

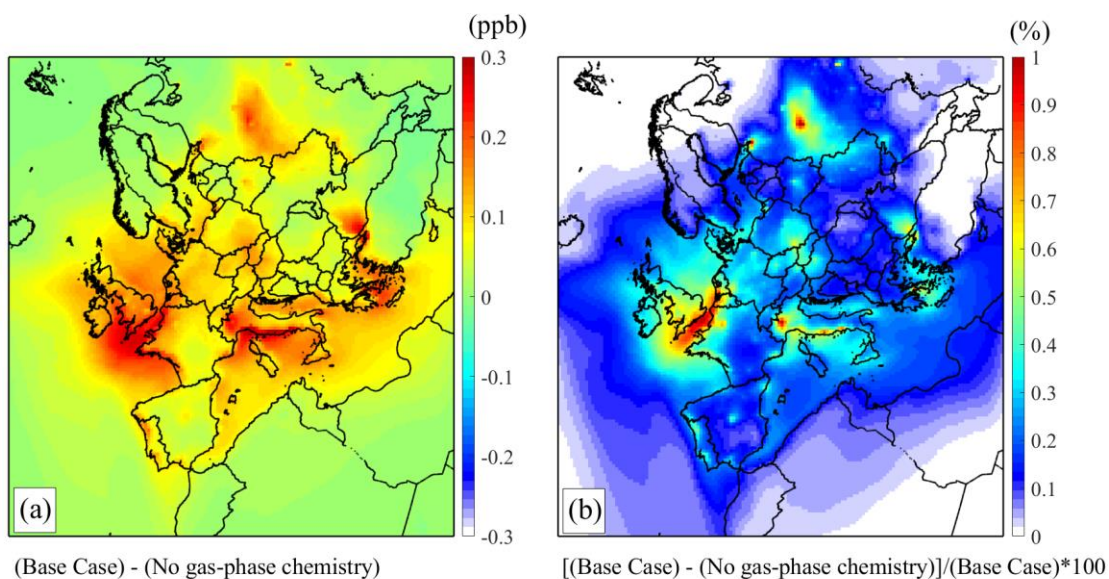


Figure S11: (a) Absolute and (b) percentage differences between the average ground-level concentrations of O_3 predicted in the “base case” and in the “no gas-phase chemistry” simulations.

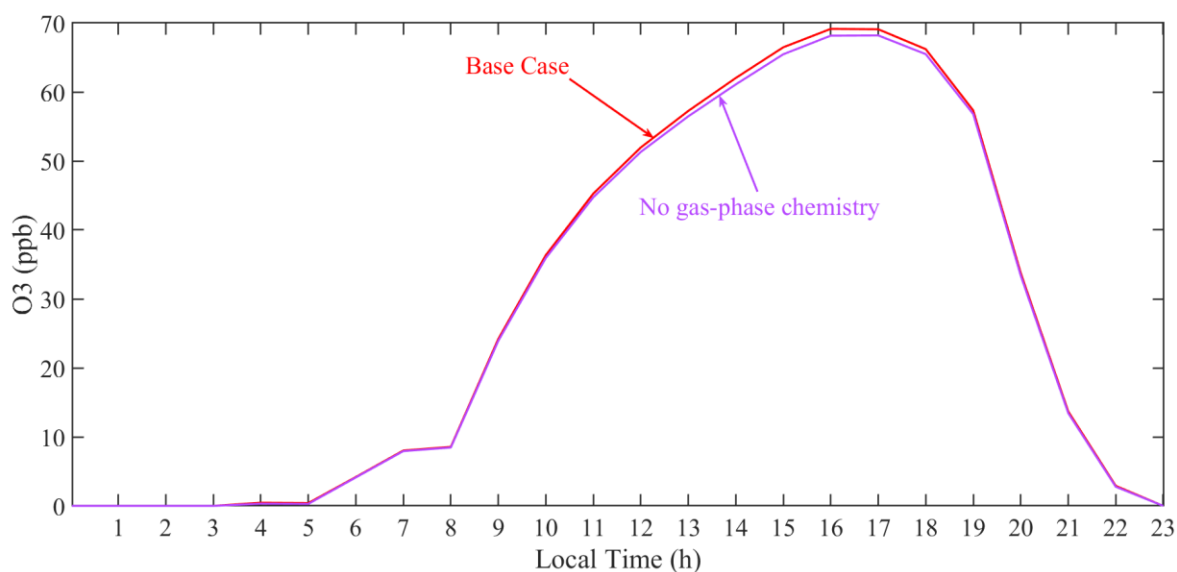


Figure S12: Predicted ground-level ozone concentrations by PMCAMx (“base case” test), PMCAMx-iv (“new IVOC scheme” test) and the “no gas-phase chemistry” sensitivity test over Milan (Italy) on the 8th of May 2008.

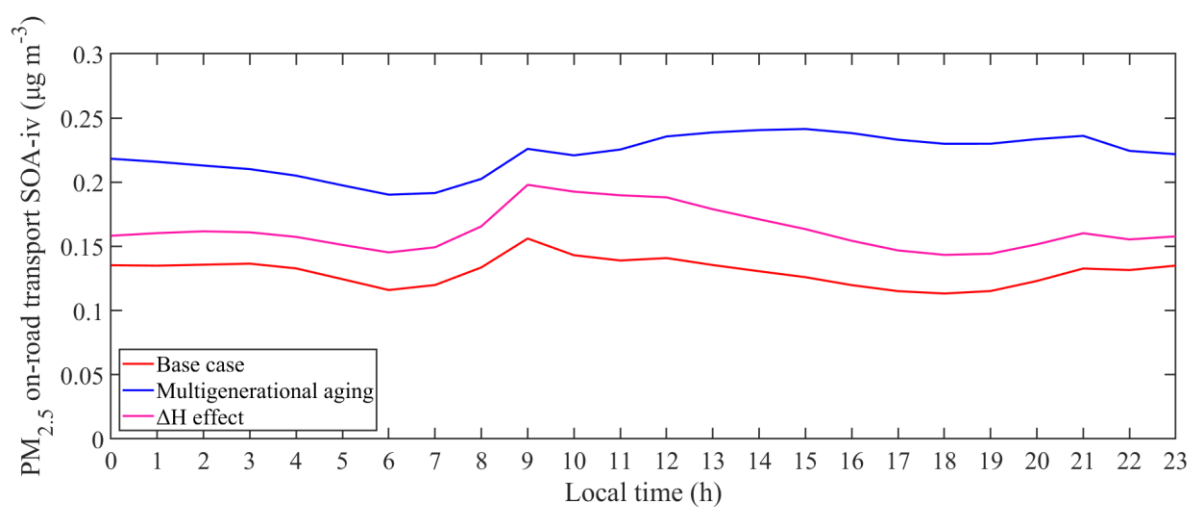


Figure S13: Diurnal profile of the PM_{2.5} ground-level on-road transport SOA-iv concentrations over Paris predicted by the “base case”, the “multigenerational aging” test and the “ ΔH effect” test.

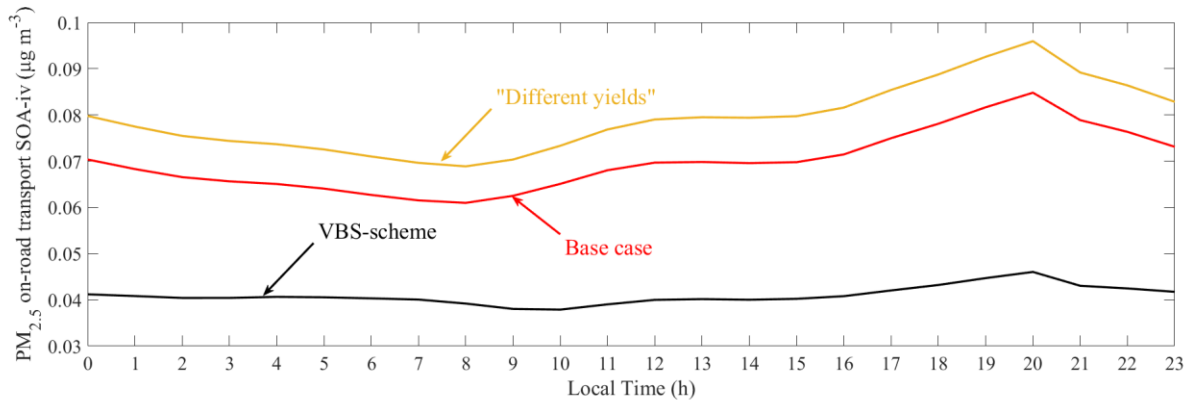


Figure S14: Diurnal profile of the PM_{2.5} ground-level on-road transport SOA-iv concentrations over Finokalia predicted by PMCAMx, PMCAMx-iv and the “different yields” sensitivity test.